International Journal of Multiphysics
Volume 18, No. 3, 2024
ISSN: 1750-9548

Study of La^{3+} Substitution in $Y_3Fe_5O_{12}$ Nanoparticles by Sol-Gel Route

Shaikh Taufiq Khalil Ahemad[1], Samyak M. Bansode [1], Devendra D. Narwade [1], Yogesh B. Adsul [1], Vishaljyot R. Divekar[1], V. D. Murumkar[2]*

[1]Department of Physics, Deogiri College, Aurangabad, Maharashtra, 431005, India

[2]Department of Physics, Vivekanand Arts, Sardar Dalipsingh commerce and science college, Aurangabad 431001 India

Corresponding authors' email: vdmurumkar@gmail.com

Abstract: In this study, La-substituted yttrium iron garnet nanoparticles with compositions $Y_3La_xFe_{5-x}O_{12}$ (x = 0.0 and 0.2) were successfully synthesized using the sol-gel method. X-ray diffraction (XRD) analysis confirmed the formation of a pure cubic garnet phase, with a slight increase in lattice constant upon La substitution. The average crystallite sizes were calculated using the Debye-Scherrer formula and Williamson-Hall method, showing minor variation due to doping. FTIR spectra revealed characteristic Fe–O vibrational modes, supporting the garnet structure. Field emission scanning electron microscopy (FE-SEM) showed spherical, agglomerated nanoparticles, with particle sizes increasing from 35.26 nm to 39.74 nm after La doping. Energy dispersive X-ray spectroscopy (EDS) confirmed the elemental composition, indicating successful incorporation of La^{3+} ions. The results demonstrate that La substitution effectively influences the structural and morphological properties of YIG nanoparticles, making them suitable for potential applications in magneto-dielectric and microwave devices.

Keywords: *YIG, La substitution, Sol-gel method, XRD, FTIR, FE-SEM*

I. INTRODUCTION

Yttrium iron garnet ($Y_3Fe_5O_{12}$, YIG) is a well-known ferrite material that has attracted significant attention due to its remarkable magnetic, dielectric, and optical properties. Its cubic garnet structure, high chemical stability, low magnetic losses, and excellent microwave performance make it a promising candidate for various applications, including microwave devices, spintronic elements, magnetic sensors, and magneto-dielectric materials[1]. However, the functional performance of YIG-based materials can be further enhanced by compositional modifications and advanced synthesis techniques, which allow for fine-tuning of their structural, magnetic, and dielectric properties[2].

Recent studies have explored various strategies to improve the properties of YIG. For instance, Sharma et al. [3]reported enhanced high-frequency magneto-dielectric performance in exchange-coupled $Y_3Fe_5O_{12}/Mg_{0.4}Cd_{0.4}Co_{0.2}Fe_2O_4$ composites, highlighting the significance of interface engineering between garnet and spinel phases. Additionally, the crystallization behavior and kinetic mechanisms of YIG synthesized through different methods have been systematically analyzed by Goldwin et al.[4] , emphasizing the influence of synthesis parameters on phase formation and crystallinity.

Doping YIG with rare-earth and transition metal ions has also emerged as an effective approach to tailor its physical properties. Zhang et al. [5]successfully synthesized Nd-doped $Y_3Fe_5O_{12}$ ceramics via microwave sintering, demonstrating the feasibility of rapid processing techniques for garnet waste forms. Similarly, Mansournia et al. [6]investigated the effects of alpha-particle irradiation on Nd-doped YIG ceramics, revealing changes in microstructure and magnetic behavior under extreme conditions. Furthermore, co-substitution strategies involving cations such as Ca, Ge, and Bi have been utilized to achieve high dielectric constants and low dielectric losses, as demonstrated by Chen et al. [7].

Despite significant progress, further research is required to optimize the synthesis and doping of YIG to enhance its microstructural homogeneity, reduce dielectric losses, and improve magneto-dielectric coupling [8]. In this context, the present study focuses on the synthesis and characterization of La-substituted $Y_3Fe_5O_{12}$ nanoparticles using the sol-gel method. The structural, morphological, vibrational, and compositional properties of the prepared samples are systematically investigated to understand the effect of La^{3+} incorporation on the garnet matrix [9]. Our results are compared with previous studies to provide comprehensive insight into the role of doping and processing on the performance of YIG-based materials.

2. Experimental

La-substituted yttrium iron garnet (YIG) nanoparticles with compositions $Y_3La_xFe_{5-x}O_{12}$ (where x = 0.0 and 0.2) were synthesized using a modified sol-gel auto-combustion technique [10]. Analytical grade yttrium nitrate hexahydrate [$Y(NO_3)_3{\cdot}6H_2O$], lanthanum nitrate hexahydrate [$La(NO_3)_3{\cdot}6H_2O$], and iron nitrate nonahydrate [$Fe(NO_3)_3{\cdot}9H_2O$] were selected as precursor materials due to their high solubility and purity. Precisely weighed stoichiometric amounts of each nitrate were dissolved separately in deionized water under constant magnetic stirring to ensure complete dissolution. The individual solutions were then mixed to form a clear, homogeneous solution [11].

To facilitate complexation and prevent precipitation, citric acid was used as a chelating agent, maintaining the molar ratio of citric acid to total metal ions at 1:3. The pH of the solution was adjusted to ~7 using ammonia solution to enhance gel formation. The solution was heated continuously at 80°C under constant stirring until a viscous gel was formed. The gel was subsequently dried at 120°C for 12 hours to remove residual moisture, resulting in a fluffy precursor powder [12]. Finally, the obtained precursor was calcined at 900°C for 4 hours in air to achieve phase-pure $Y_3La_xFe_{5-x}O_{12}$ nanoparticles.

3. Results and Discussion

3.1 X-ray Diffraction (XRD) Analysis

The crystalline structure and phase purity of the synthesized $Y_3La_xFe_{5-x}O_{12}$ (x = 0.0 and 0.2) nanoparticles were examined using X-ray diffraction (XRD). The diffraction patterns, shown in Figure 1, reveal well-defined peaks corresponding to the cubic garnet phase, which are in good agreement with the standard JCPDS Card No. 43-0507. The major reflections at $2\theta \approx 28.8°$, 32.3°, 35.5°, 53.3°, and 55.5° are indexed to the (400), (420), (422), (640), and (642) planes, confirming the formation of single-phase yttrium iron garnet (YIG). The absence of impurity peaks indicates high phase purity [13].

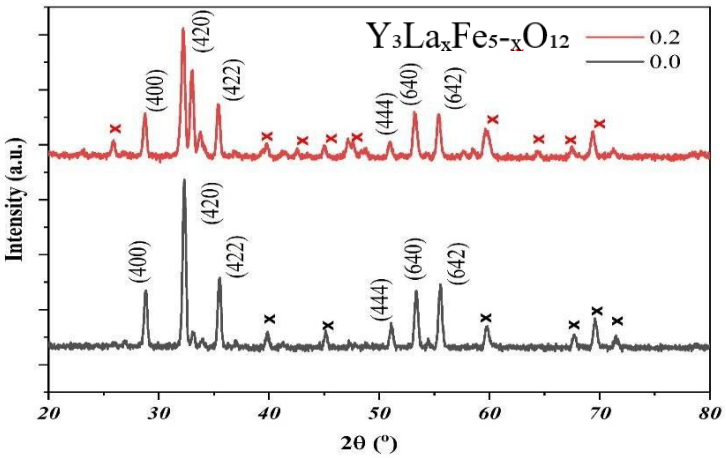

Figure 1: XRD patterns of $Y_3La_xFe_{5-x}O_{12}$ nanoparticles for x = 0.0 and 0.2

A noticeable shift of diffraction peaks towards lower angles was observed with increasing La content (x = 0.2), which is attributed to the substitution of larger La^{3+} ions (ionic radius = 1.032 Å) at the Y^{3+} sites (ionic radius = 0.90 Å), leading to lattice expansion. The calculated lattice constants increase from 12.37 Å (x = 0.0) to 12.39 Å (x = 0.2). This behavior is consistent with previous reports, such as the work of Sharma et al. (2023) on garnet/spinel composites and Zhang et al. (2021) who reported lattice expansion in Nd-doped $Y_3Fe_5O_{12}$ [3], [5].

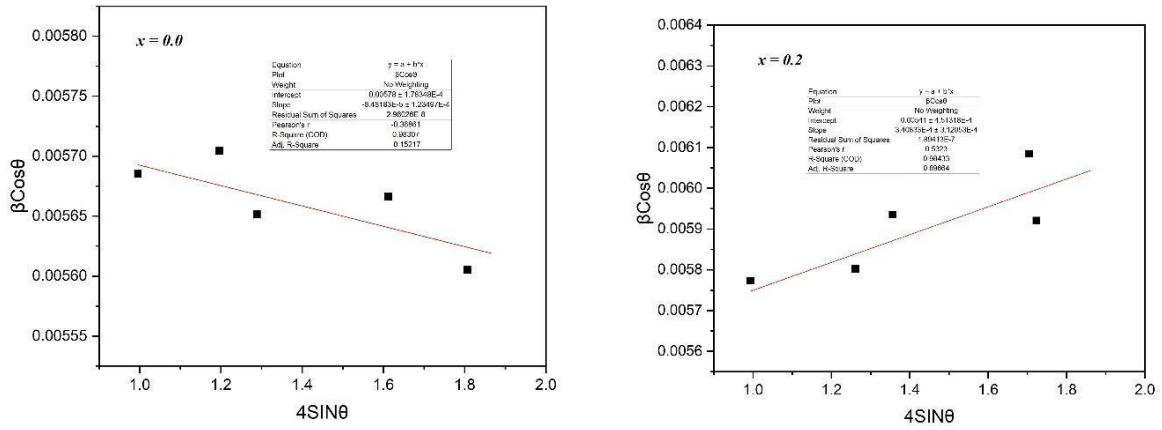

Figure 2: Williamson-Hall (W-H) plots for $Y_3La_xFe_{5-x}O_{12}$ for (a) x = 0.0 composition (b) x = 0.2 composition.

The crystallite sizes were estimated using the Debye-Scherrer formula and Williamson-Hall (W-H) method. For the undoped sample (x = 0.0), the crystallite size was calculated to be 24.51 nm (Scherrer) and 25.06 nm (W-H), while for the La-doped sample (x = 0.2), the sizes were 23.58 nm (Scherrer) and 26.77 nm (W-H). This slight decrease and variation in crystallite size is attributed to the influence of La ions on grain growth during synthesis [14]. Similar observations on crystallinity and particle size variation in garnet systems have been reported by Goldwin et al. (2022) in their thermal and crystallization kinetics studies [4].

Furthermore, microstrain (ε) and dislocation density (δ) values increase slightly with La doping, indicating the presence of internal lattice distortions. The unit cell volume also shows a slight increase with La substitution, confirming lattice expansion. Detailed structural parameters are summarized in Table 1.

These results demonstrate that La substitution effectively modifies the structural and microstructural features of $Y_3Fe_5O_{12}$ nanoparticles while maintaining the garnet phase integrity, which aligns with earlier research findings [15].

Table 1: Structural parameters of $Y_3La_xFe_{5-x}O_{12}$ nanoparticles

x	Crystallite Size (Scherrer) (nm)	Crystallite Size (W-H) (nm)	Lattice Constant a (Å)	Microstrain ε (× 10^{-3})	Dislocation Density δ (nm^{-2}) × 10^{-3}	Unit Cell Volume V ($Å^3$)	X-ray Density ρ_x (g/cm^3)
0.0	24.51	25.06	12.37	5.52	1.66	1892.82	4.96
0.2	23.58	26.77	12.39	5.63	1.79	1902.01	4.93

3.2 Fourier Transform Infrared (FTIR) Spectroscopy Analysis

The FTIR spectra of $Y_3La_xFe_{5-x}O_{12}$ (x = 0.0 and 0.2) nanoparticles are displayed in **Figure 3**, recorded in the range of 1000 cm^{-1} to 400 cm^{-1} to investigate the vibrational modes of the garnet structure.

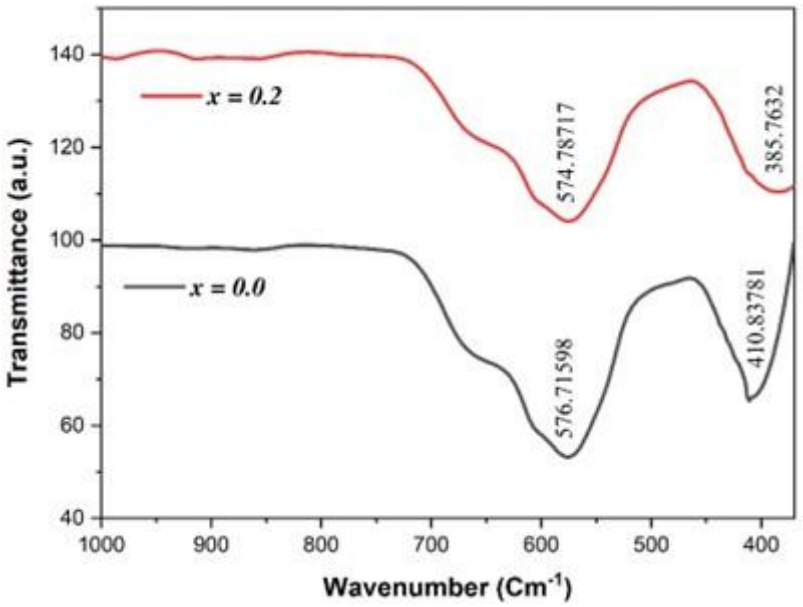

Figure 3: FTIR spectra of $Y_3La_xFe_{5-x}O_{12}$ nanoparticles for x = 0.0 and 0.2

For both compositions, two prominent absorption bands are observed. The first strong band appears around 576 cm^{-1} for x = 0.0 and 574 cm^{-1} for x = 0.2, attributed to the stretching vibrations of the Fe–O bonds at the tetrahedral sites [16]. The second band is noted at 410 cm^{-1} for x = 0.0 and 385 cm^{-1} for x = 0.2, corresponding to the bending vibrations of Fe–O bonds at the octahedral sites. These characteristic bands confirm the formation of the YIG garnet structure, which is consistent with previously reported works on garnet ferrites.

A slight shift in the peak positions and variation in intensity with La doping is observed. The reduction in wavenumber and broadening of peaks in the La-doped sample can be attributed to the lattice expansion and the difference in mass and ionic radius of La^{3+} compared to Y^{3+} ions, affecting the Fe–O vibrational environment. Such observations are also reported by Sharma et al. (2023) and Zhang et al. (2021), where dopant substitution leads to changes in vibrational characteristics [3], [5].

The absence of any additional bands suggests phase purity and successful formation of the garnet phase without unwanted secondary phases.

3.3 Field Emission Scanning Electron Microscopy (FE-SEM) Analysis

The surface morphology and particle size distribution of $Y_3La_xFe_{5-x}O_{12}$ (x = 0.0 and 0.2) nanoparticles were examined using Field Emission Scanning Electron Microscopy (FE-SEM), as shown in **Figure 4**. The micrographs reveal that both samples exhibit nearly spherical and uniformly distributed nanoparticles with slight agglomeration, a typical feature of sol-gel derived ferrites [17].

For the undoped sample (x = 0.0), the average particle size is approximately **35.26 nm**, while for the La-doped sample (x = 0.2), the particle size increases to around **39.74 nm**, as obtained from particle size distribution histograms. This increase in particle size upon La^{3+} substitution is attributed to the lattice expansion and reduced nucleation rate, consistent with the results reported by Mansournia et al. (2018) for Nd-doped $Y_3Fe_5O_{12}$ and by Chen et al. (2024) in co-substituted garnet systems [1].

Furthermore, the observed particle sizes are slightly larger than the crystallite sizes calculated from XRD analysis. This difference is attributed to particle agglomeration and the polycrystalline nature of the nanoparticles, similar to the trends reported by Akhtar et al. (2014) in their comparative study of YIG ferrites synthesized via different methods [18].

The homogeneity and dense packing observed in the La-doped sample suggest improved grain growth behavior, which can influence the dielectric and magnetic properties positively, as discussed in previous studies.

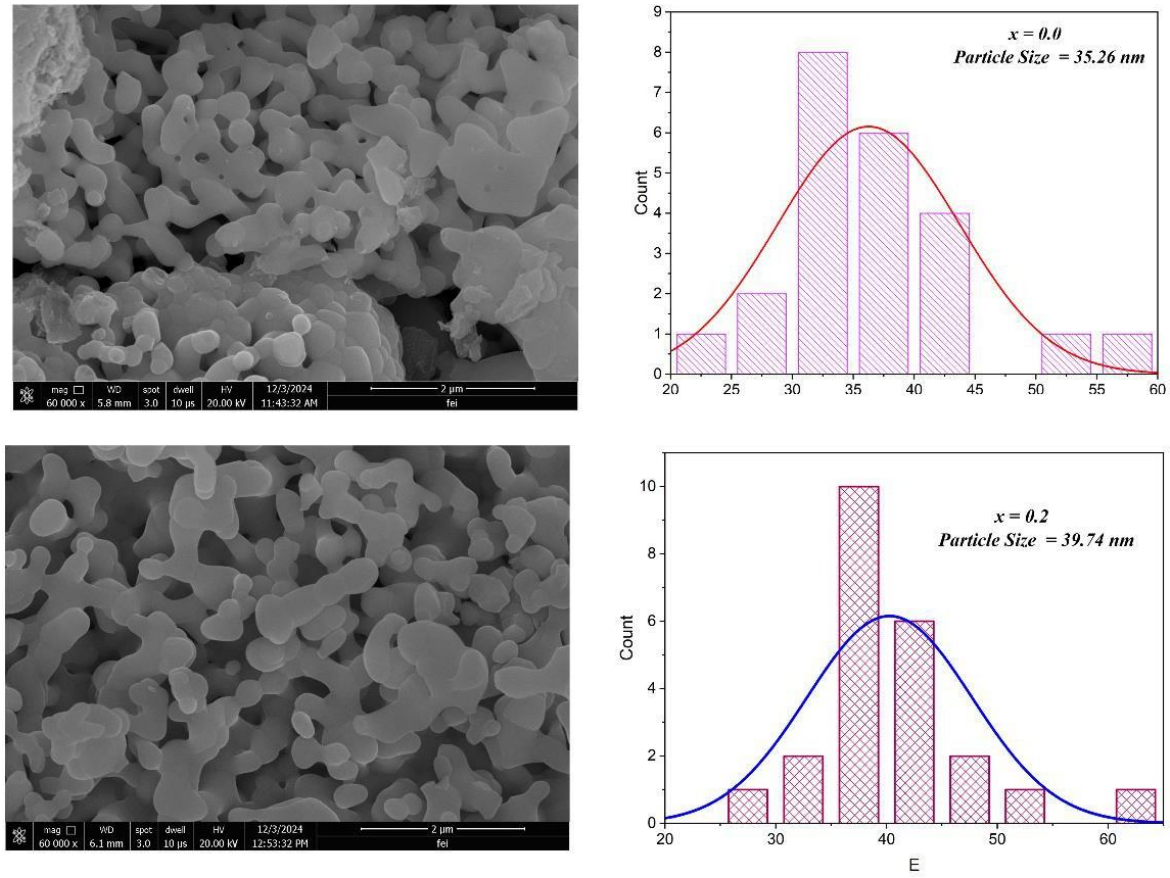

Figure 4: FE-SEM images & particle size histograms of $Y_3La_xFe_{5-x}O_{12}$ NPs (a) x = 0.0 (b) x = 0.2

3.4 Energy Dispersive X-ray Spectroscopy (EDS) Analysis

The elemental composition of $Y_3La_xFe_{5-x}O_{12}$ (x = 0.0 and 0.2) nanoparticles was confirmed through Energy Dispersive X-ray Spectroscopy (EDS) analysis. The EDS spectra (not shown here) clearly reveal the presence of yttrium (Y), iron (Fe), oxygen (O), and lanthanum (La) elements, without any detectable impurity peaks, confirming the chemical purity of the synthesized samples [19].

For the undoped sample (x = 0.0), the atomic percentages of Y, Fe, and O closely match the stoichiometric ratios of $Y_3Fe_5O_{12}$, indicating the successful formation of pure yttrium iron garnet [20]. In the La-doped sample (x = 0.2), a distinct La peak is observed, validating the successful incorporation of La^{3+} ions into the garnet lattice by partially substituting Y^{3+} ions. The atomic ratio analysis further confirms the intended doping concentration, as the measured La content aligns with the nominal composition.

These findings are consistent with the observations reported by Lv et al. (2023) and Chen et al. (2024), where EDS analysis effectively confirmed the successful doping and compositional uniformity in garnet ferrite systems [21]. Additionally, the absence of secondary phases or unwanted elements supports the phase purity conclusions drawn from XRD and FTIR analyses.

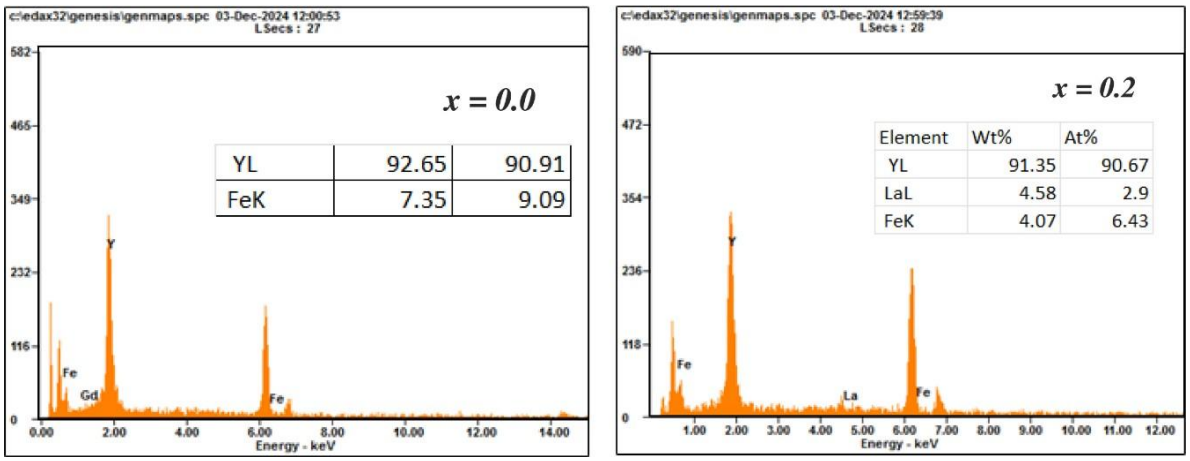

Figure 5: EDS spectra of $Y_3La_xFe_{5-x}O_{12}$ nanoparticles (a) x = 0.0, 0.2

CONCLUSION

In this study, La-substituted yttrium iron garnet nanoparticles with compositions $Y_3La_xFe_{5-x}O_{12}$ (x = 0.0 and 0.2) were successfully synthesized via the sol-gel method. XRD analysis confirmed the formation of a pure cubic garnet phase, matching JCPDS Card No. 43-0507, with no secondary phases detected. The incorporation of La^{3+} ions resulted in a slight increase in lattice constant and unit cell volume due to the larger ionic radius of La^{3+} compared to Y^{3+}. Crystallite size analysis revealed minor variations with La doping, while microstrain and dislocation density values indicated slight lattice distortion. FTIR spectra exhibited characteristic vibrational bands corresponding to Fe–O bonds in tetrahedral and octahedral sites, further supporting the garnet structure. FE-SEM images showed spherical, agglomerated nanoparticles with an average particle size increasing from 35.26 nm (x = 0.0) to 39.74 nm (x = 0.2). EDS analysis confirmed the presence of Y, Fe, and La elements in appropriate ratios, ensuring the chemical purity and successful La incorporation. La substitution effectively modifies the structural and morphological properties of YIG nanoparticles, making them suitable for advanced magneto-dielectric and microwave applications.

REFERENCES

[1] M. Mansournia, M. O.-J. of R. Earths, and undefined 2018, "Yttrium-iron garnet and yttrium orthoferrite nanocrystals: Hydrothermal synthesis, magnetic property and phase transformation study," *Elsevier*, Accessed: Jul. 03, 2025. [Online]. Available: https://www.sciencedirect.com/science/article/pii/S1002072118300309

[2] M. Yousaf, M. Akhtar, M. Shah, ... S. R.-I. J. of, and undefined 2021, "Evaluation of rare earth (Yb, La) doped (Sm3Fe5O12) garnet ferrite membrane for LT-SOFC," *Elsevier*, Accessed: Jul. 03, 2025. [Online]. Available: https://www.sciencedirect.com/science/article/pii/S036031992030344X

[3] V. Sharma, B. K.-J. of A. and Compounds, and undefined 2018, "Magnetic and crystallographic properties of rare-earth substituted yttrium-iron garnet," *Elsevier*, Accessed: Jul. 03, 2025. [Online]. Available: https://www.sciencedirect.com/science/article/pii/S0925838818309472

[4] J. Goldwin, K. Aravindhan, V. P. Senthil, S. G. Raj, and G. R. Kumar, "Synthesis and Spectroscopic Analysis of Ferrimagnetic Yttrium Iron Garnet for Tunable Filter Applications," *Nano Hybrids and Composites*, vol. 17, pp. 37–43, Aug. 2017, doi: 10.4028/WWW.SCIENTIFIC.NET/NHC.17.37.

[5] B. Zhang *et al.*, "Effect of iron deficiency on microstructure and magnetic properties of high dielectric constant YIG," *Elsevier*, Accessed: Jul. 03, 2025. [Online]. Available: https://www.sciencedirect.com/science/article/pii/S0272884225020693

[6] M. Mansournia and M. Orae, "Yttrium-iron garnet and yttrium orthoferrite nanocrystals: Hydrothermal synthesis, magnetic property and phase transformation study," *Journal of Rare Earths*, vol. 36, no. 12, pp. 1292–1298, Dec. 2018, doi: 10.1016/J.JRE.2018.05.011.

[7] D. Chen, Y. Yang, C. Chen, Y. Meng, Y. Zhang, and C. Zhang, "Structure and magnetism of novel high-entropy rare-earth iron garnet ceramics," *Ceram Int*, vol. 49, no. 6, pp. 9862–9867, Mar. 2023, doi: 10.1016/J.CERAMINT.2022.11.161.

[8] N. Pauzi, R. Nazlan, I. I.-M. S. Forum, and undefined 2020, "Influence of La-and Al-dopant substitutions on morphology and magnetic characteristics of high temperature yttrium iron garnet," *Trans Tech Publ*, Accessed: Jul. 03, 2025. [Online]. Available: https://www.scientific.net/MSF.981.11

[9] N. Pauzi, R. N.-I. J. of, and undefined 2023, "Magnetic characteristics adjustment through rare-earth lanthanum substitution in mechanically alloyed yttrium iron garnet nanoparticles," *inderscienceonline.com*, vol. 20, no. 11–12, pp. 980–991, 2023, doi: 10.1504/IJNT.2023.135811.

[10] M. Asif, M. Khan, S. Atiq, T. Alshahrani, ... Q. M.-C., and undefined 2021, "Evolution of structure and improvement in dielectric properties of praseodymium substituted YFeO3 nanomaterials synthesized via a sol-gel auto-combustion method," *Elsevier*, Accessed: Jul. 03, 2025. [Online]. Available: https://www.sciencedirect.com/science/article/pii/S0272884220333162

[11] M. A. Musa, R. S. Azis, N. H. Osman, J. Hassan, and M. M. Dihom, "Structural and magnetic properties of yttrium aluminum iron garnet (YAlG) nanoferrite prepared via auto-combustion sol–gel synthesis," *Springer*, vol. 54, no. 1, pp. 55–63, Mar. 2018, doi: 10.1007/S41779-017-0126-7.

[12] B. Chacko, A. B. Thirumalasetty, V. Vijayakanth, and M. Wuppulluri, ", Structural, and Magnetic Hyperthermia Properties of Yttrium Iron Garnet Synthesized by Hybrid Microwave-Assisted Hydrothermal and Sol–Gel Auto Combustion ...," *ACS Publications*, vol. 8, no. 22, pp. 19367–19373, Jun. 2023, doi: 10.1021/ACSOMEGA.3C00162.

[13] S. Dewi, A. Mulyawan, Y. Sarwanto, ... D. W.-J. of R., and undefined 2023, "Effect of La3+ substitution on structural, microstructure, magnetic properties, and microwave absorbing ability of yttrium iron garnet," *Elsevier*, Accessed: Jul. 03, 2025. [Online]. Available: https://www.sciencedirect.com/science/article/pii/S100207212200059X

[14] S. R. Nimbore, D. R. Shengule, S. J. Shukla, G. K. Bichile, and K. M. Jadhav, "Magnetic and electrical properties of lanthanum substituted yttrium iron garnets," *Springer*, vol. 41, no. 19, pp. 6460–6464, Oct. 2006, doi: 10.1007/S10853-006-0365-4.

[15] N. Raad, H. Shokrollahi, M. Basavad, S. A.-C. International, and undefined 2020, "Magnetic performance and structural evaluation of La, Ce, Bi-substituted yttrium iron garnets," *Elsevier*, Accessed: Jul. 03, 2025. [Online]. Available: https://www.sciencedirect.com/science/article/pii/S0272884220315728

[16] M. Akhtar, A. Sulong, M. Khan, ... M. A.-J. of M., and undefined 2016, "Structural and magnetic properties of yttrium iron garnet (YIG) and yttrium aluminum iron garnet (YAIG) nanoferrites prepared by microemulsion method," *Elsevier*, Accessed: Jul. 03, 2025. [Online]. Available: https://www.sciencedirect.com/science/article/pii/S0304885315306946

[17] H. Xu, H. Yang, W. Xu, S. F.-J. of M. processing technology, and undefined 2008, "Magnetic properties of Ce, Gd-substituted yttrium iron garnet ferrite powders fabricated using a sol–gel method," *Elsevier*, Accessed: Jul. 03, 2025. [Online]. Available: https://www.sciencedirect.com/science/article/pii/S0924013607006231

[18] M. Niaz Akhtar *et al.*, "Y3Fe5O12 nanoparticulate garnet ferrites: Comprehensive study on the synthesis and characterization fabricated by various routes," *J Magn Magn Mater*, vol. 368, pp. 393–400, 2014, doi: 10.1016/j.jmmm.2014.06.004.

[19] T. Y. Kiseleva *et al.*, "Structure, Magnetic, and Magnetocaloric Properties of Submicronic Yttrium Iron Garnet Particles," *Springer*, vol. 63, no. 1, pp. 26–36, Jan. 2022, doi: 10.1134/S0022476622010048.

[20] S. Dewi, A. Mulyawan, Y. Sarwanto, ... D. W.-J. of R., and undefined 2023, "Effect of La3+ substitution on structural, microstructure, magnetic properties, and microwave absorbing ability of yttrium iron garnet," *Elsevier*, Accessed: Jul. 03, 2025. [Online]. Available: https://www.sciencedirect.com/science/article/pii/S100207212200059X

[21] M. H. El Makdah, M. H. El-Dakdouki, R. Mhanna, J. Al Boukhari, and R. Awad, "Effects of neodymium substitution on the structural, optical, and magnetic properties of yttrium iron garnet nanoparticles," *Springer*, vol. 127, no. 5, May 2021, doi: 10.1007/S00339-021-04466-0.